

Defect motion in a quantum solid with spin: hcp ^3He

Zhi Gang Cheng and John Beamish

Department of Physics, University of Alberta, Edmonton, Alberta, Canada T6G 2E1

(Received 13 January 2017; revised manuscript received 21 April 2017; published 30 May 2017)

Defect motion in solid helium has a unique quantum nature due to the large zero-point motion of helium atoms, which allows vacancies and isotopic impurities to tunnel and move ballistically. Recent shear modulus experiments showed that dislocations are also extraordinarily mobile in solid ^4He . The lighter isotope, ^3He , has even larger zero-point motion and an extra degree of freedom—nuclear spin—which can affect defect motion. We have measured the shear modulus of hcp solid ^3He to probe the motion of dislocations and isotopic impurities. We observed a crossover between stiff and soft states, due to ^4He impurities which immobilize dislocations at low temperatures. In contrast to solid ^4He , the impurities in hcp ^3He act as *static* pinning sites because of the disordered configuration of ^3He nuclear spins. In addition, we observed an unexpected dissipation that increased rapidly at low frequencies, indicating a strong interaction between nuclear spins and moving dislocations.

DOI: [10.1103/PhysRevB.95.180103](https://doi.org/10.1103/PhysRevB.95.180103)

The behavior of defects in a quantum solid such as helium differs from that in a conventional solid due to the atoms' large zero-point motion. Vacancies and impurities exhibit quantum diffusion and propagate freely in solid ^4He , even at low temperatures. Dislocations in hcp ^4He crystals can glide without dissipation at low temperatures, reducing the shear modulus by as much as 90%, an effect referred to as “giant plasticity” [1]. Such an extremely high mobility of dislocations not only reflects the quantum nature of solid helium, but also provides a unique model for studies of material science. Even more dramatic effects have been predicted, including zero-point vacancies and supersolidity in ^4He crystals [2]. Although recent experiments have shown that the apparent mass decoupling seen in torsional oscillator measurements [3,4] is due to elastic effects associated with dislocations rather than supersolidity [5,6], numerical simulations suggest that the dislocations could have superfluid cores [7]. Superflow through a network of dislocations has been proposed as an explanation of unusual mass flow through a superfluid-solid-superfluid junction [8]. Such superfluid dislocations—unique to ^4He as a boson—could also “superclimb” [9–11], providing a different mechanism of plastic deformation.

Quantum effects are even more important in crystals of ^3He . Its smaller mass and larger zero-point motion give ^3He a more open bcc crystal structure at pressures below 110 bar, with higher exchange frequencies and lower vacancy energies. ^3He also has nuclear spin, which gives it a rich phase diagram with ordered magnetic phases at very low temperatures. In the paramagnetic phase above 1 mK, the spins are disordered but short-range spin correlations remain, with measurable effects, for example, in specific heat measurements [12], extending well above 100 mK. Spin disorder in the paramagnetic phase destroys the coherent tunneling responsible for the ballistic propagation of “vacancions” and “impuritons” in solid ^4He . A recent plastic flow experiment provided some evidence of quantum vacancy motion at low temperatures in bcc ^3He [13], but NMR techniques used to study the quantum diffusion of ^3He impurities in ^4He cannot be applied directly to spinless ^4He impurities or vacancies, so less is known about their motions in solid ^3He . Dislocation motion is very sensitive to pinning by impurities, so elastic measurements provide a probe of the mobility of ^4He atoms in solid ^3He . A gliding dislocation

also rearranges spin configurations, which provides a different damping mechanism that may affect the elastic behavior. Early ultrasonic measurements [14,15] showed that dislocations and impurities affect longitudinal sound speeds in bcc and hcp ^3He , as well as in hcp ^4He , but the high (MHz) frequencies complicated their interpretations. More recent measurements [16] showed that softening due to dislocations in hcp ^4He also exists in ^3He , but the measurements were limited to a single frequency (2000 Hz) and did not include the accompanying dissipation. In this Rapid Communication we focus on the high pressure hcp phase and report measurements of the shear modulus μ and elastic dissipation $1/Q$ of solid ^3He as functions of temperature, frequency, and strain amplitude. This comprehensive study of the hcp phase allows us to compare directly to the Bose solid, hcp ^4He , where recent experiments have produced a detailed picture of dislocations and their interactions with isotopic impurities [1,17–20].

The experimental setup is similar to that used for solid ^4He [1,17]. Since the amount of available ^3He was limited, we built a BeCu cell with a smaller volume of 0.79 cm³ and a surface area of 10 cm². The gap between the two Pb(ZrTi)O₃ (PZT) shear transducers was 0.95 mm. Most samples were grown from the highest purity ^3He available (containing 1.35 ppm ^4He) and a few were grown with 50 ppm ^4He . At such low ^4He concentrations, phase separations should only appear below 50 and 70 mK, respectively [21]. Also at these concentrations there is enough ^4He to coat the surface with most of them left in the bulk solid [22]. Measurements of the shear modulus and dissipation were made at frequencies between 22 and 5402 Hz, and strain amplitudes from $\epsilon = 9.4 \times 10^{-8}$ (in the linear regime where results were independent of strain amplitude) up to about 9.4×10^{-7} . Technical details of the measurements are provided in the Supplemental Material (SM) [22].

Figure 1(a) shows the temperature dependence of the shear modulus of an hcp ^3He sample at different frequencies, measured at low strain amplitude. The sample was a polycrystal grown using the blocked capillary method. Its final pressure was around 119 bar, in the hcp phase at low temperatures. The modulus decreased by $\sim 30\%$ from 25 to 500 mK, comparable to typical changes for polycrystalline hcp ^4He [17,23] and much larger than what nondislocation mechanisms can produce. The crossover between stiff and soft states is broader and

extends to higher temperatures than in ^4He , probably because of the higher impurity concentration in the ^3He samples (1.35 ppm of ^4He , compared to 0.12 ppm of ^3He in the ^4He crystal). In ^4He , the crossover shifts to higher temperature for larger impurity concentration [17]: At 2000 Hz, it would occur around 200 mK for a ^3He concentration of 1.35 ppm. Most of the shear modulus change happens well above 50 mK, the estimated phase separation temperature [21], and the results show no time dependence or hysteresis during thermal cycling, features of phase separation in solid helium [15,24]. The stiffening cannot be ascribed to phase separation, but must be due to binding of ^4He impurities onto dislocations. We also performed measurements on samples with 50 ppm ^4He [22]. The softening in the less pure ^3He crystals occurred at higher temperatures, confirming further that ^4He impurities are bound to and can immobilize dislocations in hcp ^3He , but there was no sign of phase separation in these crystals either.

There is, however, a striking difference in the frequency dependence of the modulus between ^4He and ^3He crystals: The crossover temperature depends strongly on frequency in ^4He [23] [Fig. 1(c)] but is independent of frequency in ^3He [Fig. 1(a)]. For hcp ^4He , the modulus crossover is accompanied by a dissipation peak which also shifts with frequency. Both μ and $1/Q$ are well described by a Debye relaxation process with a thermal activation energy $E_a \approx 0.7$ K [18,20,23]. For a relaxation process, the peak's magnitude scales with the modulus change and so would be expected to be about 50% larger in ^3He than in the ^4He sample. However, the dissipation is completely different in hcp ^3He . At frequencies above 802 Hz there is a peak near 100 mK with a magnitude of $\sim 2 \times 10^{-3}$, about ten times smaller than in ^4He at similar frequencies. Below 802 Hz the dissipation increases rapidly. At the lowest frequencies it has a broad maximum around 200 mK. This is in marked contrast to thermally activated relaxation peaks such as those in hcp ^4He [18,23] which move to a lower temperature as the frequency decreases. The differences in both modulus and dissipation indicate that the ^4He impurities act as *static* dislocation pinning centers in hcp ^3He , in contrast to hcp ^4He , where ^3He impurities are dragged by dislocations and produce the observed thermally activated relaxation in the modulus and dissipation [18].

In hcp ^4He , the modulus stiffening at low temperatures and the associated dissipation peaks are suppressed at large strain amplitudes, as shown in Figs. 2(c) and 2(d) [25]. This is because large stresses detach dislocations from weakly bound ^3He impurities, allowing them to move freely. This eliminates the crossover to a stiff state at low temperatures and the dissipation peak associated with the dragging of ^3He impurities in solid ^4He . Figure 2(a) shows a similar amplitude dependence of the shear modulus in hcp ^3He , indicating that a breakaway from impurities occurs at similar stresses in ^3He , as was observed in the early ultrasonic measurements [15].

The unexpected hcp ^3He dissipation behavior shown in Fig. 1(b) also has a strong amplitude dependence [Fig. 2(b)], but is quite different from that of hcp ^4He [Fig. 2(d)]. The large, broad, low frequency (22 Hz) dissipation peak seen in hcp ^3He shifts to lower temperatures and its magnitude decreases as the amplitude increases. At a higher frequency (802 Hz), the dissipation below 200 mK increases at large amplitudes, presumably because of dislocations breaking away

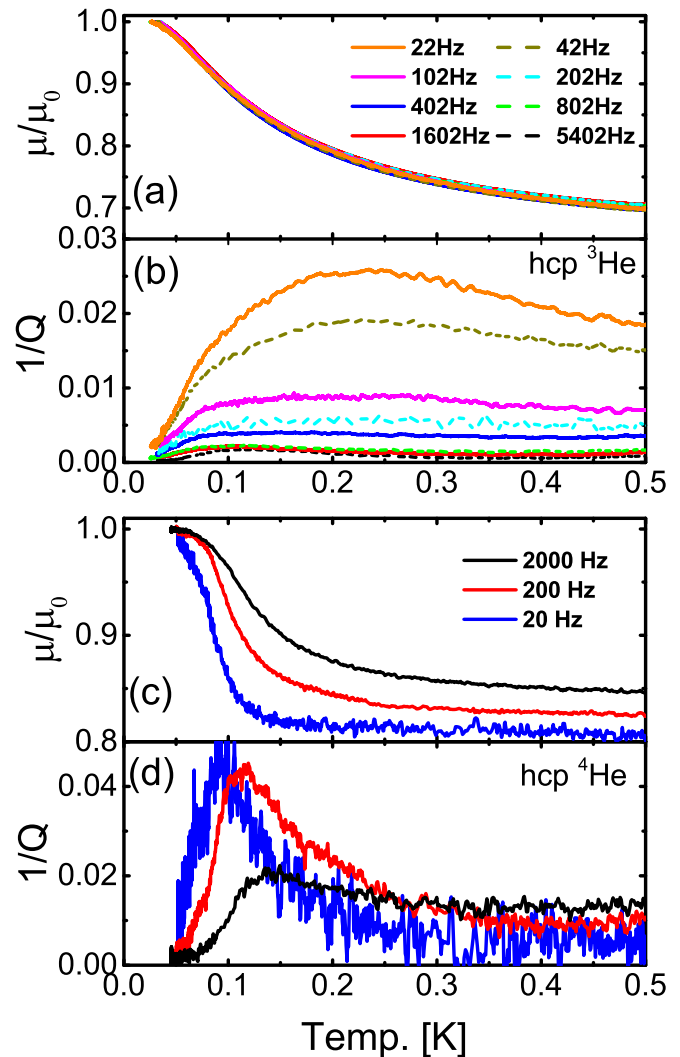


FIG. 1. (a) Shear modulus and (b) dissipation of hcp ^3He at frequencies between 22 and 5402 Hz, compared to those of (c), (d) hcp ^4He . Modulus data are normalized by their values at base temperatures μ_0 . Strain amplitude $\epsilon = 9.38 \times 10^{-8}$ for ^3He and $\epsilon < 10^{-8}$ for ^4He . ^3He data in (a) collapse onto a single curve even before normalization. ^4He data are regenerated from Ref. [23].

from the impurity pinning sites. This dissipation behavior is quite different from that in hcp ^4He , where the relaxation peaks at 200 and 2000 Hz occur at different temperatures (higher for the 2000 Hz data) but have essentially the same amplitude dependence: Both are suppressed at high amplitude but the peak temperatures are unchanged.

Although the shear modulus changes in hcp ^4He and hcp ^3He have similar magnitudes and occur over similar temperature ranges, the differences described above imply that defects behave differently in the two solids. This can be attributed to ^3He 's unique nuclear spin system. If all the spins in solid ^3He were ferromagnetically aligned, a ^4He impurity (or a vacancy) would see a periodic potential and tunneling would allow it to move ballistically, as for point defects in solid ^4He . However, ^3He is in the paramagnetic state at the temperatures of our experiments. When a ^4He impurity exchanges with a ^3He atom, the local spin arrangements (and interaction energies)

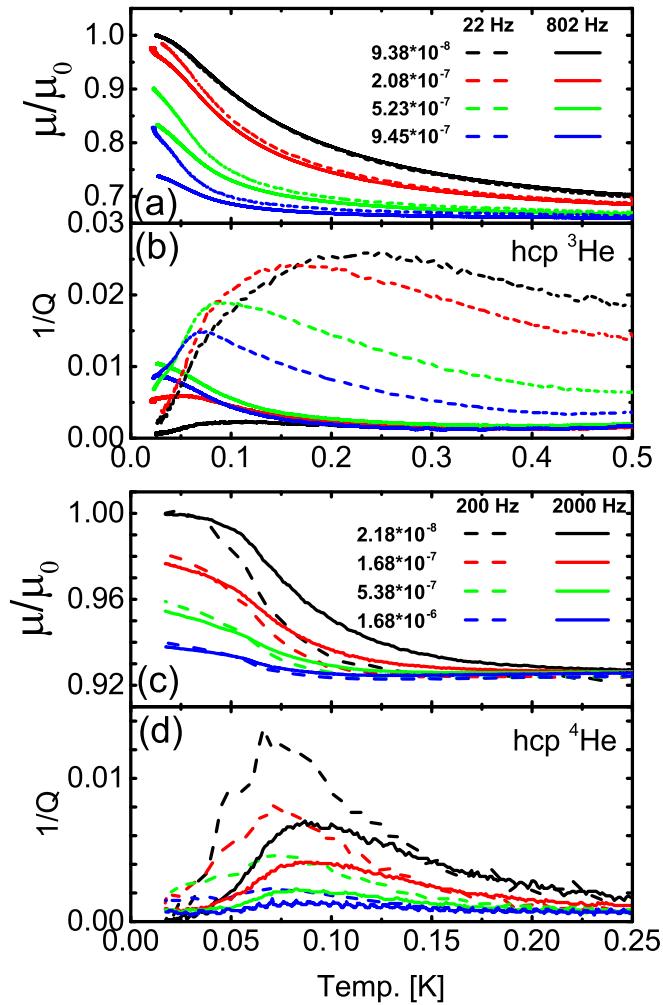


FIG. 2. Shear modulus and dissipation of hcp ^3He [(a) and (b)] and ^4He [(c) and (d)] measured at different strain amplitudes. For each sample, data at two different frequencies are presented. The modulus data are normalized by the values at base temperatures and the smallest strain amplitudes. ^4He data are regenerated from Ref. [25].

are changed, so a ^4He impurity moves in a random potential. It cannot propagate ballistically and so is much less mobile than a ^3He impurity in solid ^4He . This explains why ^4He impurities act as *static* pinning centers in hcp ^3He , in contrast to hcp ^4He where ^3He impurities move with dislocations at low speeds, damping their motion and producing the observed thermally activated relaxation behavior [18].

Dislocations produce much larger scale spin rearrangements than impurities. For example, moving edge dislocations displace atoms in the layer above their glide planes by a lattice constant (the Burgers vector b) with respect to those below. In ^3He , this rearranges neighboring spins, which raises their average interaction energy. The same dislocations are also responsible for the additional strain that reduces the crystal's shear modulus. The number of rearranged spins and the shear modulus change are proportional—both reflect the total area swept out by dislocations. If the spin interaction between nearest neighbors is $\pm J$ (for antialigned/aligned spins) then the maximum spin energy change is $12J$ for each of the atoms

in the area of the glide plane swept out by the dislocation (see SM [22] for details). The energy cost of rearranging spins is proportional to a dislocation's displacement, so the effect is analogous to a constant frictional force acting on the dislocation. At the temperatures of our experiments, the solid is in a disordered paramagnetic phase where the average interaction energy of neighboring spins is much smaller than J . It is reduced by a factor of roughly $J/k_B T$ from the value in a perfectly ordered zero temperature phase and approaches zero for completely random spins in the high temperature limit. If the dislocation motion is sufficiently slow, or the spin diffusion is sufficiently fast, all of the dislocation-induced increase in spin energy is lost during each strain cycle. The corresponding dissipation can be estimated [22] by comparing the lost spin energy to the total elastic energy $U_{\text{elastic}} = \frac{1}{2}\mu\epsilon^2$,

$$\frac{1}{Q} = \frac{1}{2\pi} \frac{\Delta U_{\text{spin}}}{U_{\text{elastic}}} = \frac{96}{\sqrt{3}\pi} \frac{\Delta\mu}{\mu_0} \frac{J}{\mu b^3 \epsilon} \frac{J}{k_B T}, \quad (1)$$

where $\Delta\mu/\mu_0$ is the fractional reduction in the shear modulus due to dislocations and ϵ is the applied strain.

The measured low frequency dissipation has most of the features predicted by Eq. (1). It decreases with increasing strain, and at high temperatures, although pinning by ^4He impurities immobilizes dislocations below 200 mK, eliminating spin damping and obscuring the intrinsic behavior. The spin friction model predicts an elastic dissipation inversely proportional to strain amplitude and independent of the measurement frequency. This is quite different from thermal phonon scattering in hcp ^4He , for which the damping force is proportional to dislocation velocity and produces an amplitude-independent dissipation proportional to frequency at high temperatures [19]. The magnitude of the estimated spin dissipation can be compared to our measurements. Using typical values for a hcp ^3He polycrystal ($\Delta\mu/\mu_0 \approx 30\%$, $\mu \approx 2 \times 10^7$ Pa, $b = 0.3$ nm, $J/k_B \approx 13$ μK [26]), the maximum spin dissipation (when $J/k_B T = 1$) at a strain $\epsilon = 9.4 \times 10^{-8}$ is $1/Q \approx 19$. Dislocations and spins would be so strongly coupled that the dislocations would be nearly immobilized. At a temperature of 100 mK, however, the spins are almost random ($J/k_B T \approx 1.3 \times 10^{-4}$), and Eq. (1) predicts a much smaller spin dissipation $1/Q \approx 2.4 \times 10^{-3}$. This is within about an order of magnitude of the measured low frequency dissipation shown in Fig. 1(b), confirming the importance of this damping mechanism. Note that our model probably underestimates the dissipation, since it neglects orientation effects in polycrystals and does not consider the multiple exchanges that are known to be important in solid helium [22]. However, the fact that the dissipation peak for 50 ppm sample [22] has the same amplitude as the 1.35 ppm sample provides further evidence that the low frequency dissipation is unrelated to impurities or phase separation, but rather is due to the motion of dislocations.

The estimation above is essentially based on a quasistatic model of dislocation dissipation. It assumes that the rearrangement of atoms by a dislocation always leaves the spins in a higher energy configuration, which will dissipate via spin exchange. However, if the spins are not mobile, they would all be restored to their original configurations when the dislocation glides in the opposite direction during a cycle of the ac strain. There would be no net energy loss during a complete oscillation.

tion and hence no net dissipation. If, however, the reconfigured spins diffuse away from the glide plane before the dislocation returns, there will be a net increase in the spin energy during each cycle. The rate at which spins diffuse away from the glide plane in hcp ^3He is roughly the exchange frequency $J/h \approx 300$ kHz [26]. At sufficiently low experimental strain frequencies, $f \ll J/h$, spins will diffuse away before the oscillating dislocations return, giving the spin dissipation of Eq. (1). At high frequencies, $f \gg J/h$, spins are frozen on the time scale of a dislocation's oscillation and we expect the dissipation associated with spin rearrangements to disappear. This sort of frequency dependence is seen in the data of Fig. 1(b), but the crossover occurs around 100 Hz, much lower than the exchange frequency J/h . At our highest frequencies, above 800 Hz, all that remains is a small dissipation peak around 0.1 K which shifts to slightly higher temperatures as the frequency increases to 5402 Hz [Fig. 1(b)]. This resembles the thermally activated behavior seen in hcp ^4He , where it is associated with impurities bound to dislocations.

There is a second frequency that may be relevant to dislocation motion, $f_P = v/b$, at which a dislocation gliding at speed v moves over the lattice's Peierls potential. The maximum speed of a dislocation loop of length L is $v = 2\pi f \frac{\pi(1-\nu)}{16b} L^2 \epsilon$ [18], where Poisson's ratio $\nu \approx 0.3$. If we assume dislocations in our sample have the same length as in ^4He polycrystals, $L \approx 60 \mu\text{m}$ [19], then for the measurements of Fig. 1 the "Peierls frequency" f_P ranges from 0.07 to 18 MHz, which spans the exchange frequency $J/h = 300$ kHz that determines whether spins can exchange in the time it takes a dislocation to move by one lattice constant. It is interesting to notice that the crossover frequency, 100 Hz, corresponds to $f_P \approx J/h$. The correlation between "Peierls frequency"

and exchange frequency suggests that spins may influence dislocation motion via short-range interaction.

To summarize, we have probed the motion of defects in hcp ^3He by measuring its shear modulus and dissipation over a wide range of temperatures, frequencies, and strain amplitudes. In sharp contrast to the case of hcp ^4He crystals, we found that isotopic impurities behave as nearly *static* dislocation pinning centers in hcp ^3He , leading to a frequency-independent shear modulus with very little dissipation at high frequencies. We also discovered an unexpected dislocation damping mechanism associated with ^3He 's nuclear spins. This produces additional dissipation at low frequencies, which decreases as the temperature, frequency, or strain amplitude increase. Dislocations and spins are strongly coupled in solid ^3He via the local atomic rearrangements that accompany dislocation motion. A simple model of this "spin friction" agrees qualitatively with the observed behavior and estimates of the expected dissipation are consistent with our measured values. Additionally, the comparison between our results for hcp ^3He and the corresponding behavior in hcp ^4He highlights the unique mobility of dislocations in the Bose solid. Similar comparisons of plastic deformation and flow in the two solids could clarify whether superfluid dislocation cores and associated phenomena such as superclimb are responsible for the giant isochoric compressibility [9–11] and low temperature flow recently observed in solid ^4He [8,27–29].

We thank Moses Chan for providing the ^3He gas from which the samples with 50 ppm ^4He was grown. This work was supported by a grant from NSERC Canada.

-
- [1] A. Haziot, X. Rojas, A. D. Fefferman, J. R. Beamish, and S. Balibar, *Phys. Rev. Lett.* **110**, 035301 (2013).
- [2] A. F. Andreev and I. M. Lifshitz, *Sov. Phys. JETP* **29**, 1107 (1969).
- [3] E. Kim and M. H. W. Chan, *Nature (London)* **427**, 225 (2004).
- [4] E. Kim and M. H. W. Chan, *Science* **305**, 1941 (2004).
- [5] J. R. Beamish, A. D. Fefferman, A. Haziot, X. Rojas, and S. Balibar, *Phys. Rev. B* **85**, 180501 (2012).
- [6] D. Y. Kim and M. H. W. Chan, *Phys. Rev. Lett.* **109**, 155301 (2012).
- [7] M. Boninsegni, A. B. Kuklov, L. Pollet, N. V. Prokof'ev, B. V. Svistunov, and M. Troyer, *Phys. Rev. Lett.* **99**, 035301 (2007).
- [8] R. B. Hallock, *J. Low Temp. Phys.* **180**, 6 (2015).
- [9] S. G. Söyler, A. B. Kuklov, L. Pollet, N. V. Prokof'ev, and B. V. Svistunov, *Phys. Rev. Lett.* **103**, 175301 (2009).
- [10] A. B. Kuklov, *Phys. Rev. B* **92**, 134504 (2015).
- [11] A. B. Kuklov, L. Pollet, N. V. Prokof'ev, and B. V. Svistunov, *Phys. Rev. B* **90**, 184508 (2014).
- [12] D. S. Greywall, *Phys. Rev. B* **15**, 2604 (1977).
- [13] A. Lisunov, V. Maidanov, V. Rubanskyi, S. Rubets, E. Rudavskii, S. Smirnov, and V. Zhuchkov, *Phys. Rev. B* **92**, 140505 (2015).
- [14] J. R. Beamish and J. P. Franck, *Phys. Rev. B* **26**, 6104 (1982).
- [15] J. R. Beamish and J. P. Franck, *Phys. Rev. B* **28**, 1419 (1983).
- [16] J. T. West, O. Syshchenko, J. R. Beamish, and M. H. W. Chan, *Nat. Phys.* **5**, 598 (2009).
- [17] J. Day and J. R. Beamish, *Nature (London)* **450**, 853 (2007).
- [18] A. Haziot, A. D. Fefferman, F. Souris, J. R. Beamish, H. J. Maris, and S. Balibar, *Phys. Rev. B* **88**, 014106 (2013).
- [19] A. Haziot, A. D. Fefferman, J. R. Beamish, and S. Balibar, *Phys. Rev. B* **87**, 060509 (2013).
- [20] F. Souris, A. D. Fefferman, H. J. Maris, V. Dauvois, P. Jean-Baptiste, J. R. Beamish, and S. Balibar, *Phys. Rev. B* **90**, 180103 (2014).
- [21] D. O. Edwards and S. Balibar, *Phys. Rev. B* **39**, 4083 (1989).
- [22] See Supplemental Material at <http://link.aps.org/supplemental/10.1103/PhysRevB.95.180103> which includes Refs. [21,30,31], for experimental details, results of samples with higher ^4He concentrations, and estimation of energy dissipation due to spin interactions.
- [23] O. Syshchenko, J. Day, and J. Beamish, *Phys. Rev. Lett.* **104**, 195301 (2010).
- [24] X. Rojas, A. Haziot, V. Bapst, S. Balibar, and H. J. Maris, *Phys. Rev. Lett.* **105**, 145302 (2010).
- [25] J. Day, Fundamental properties of quantum solid ^4He , Ph.D. thesis, University of Alberta, 2008.
- [26] R. A. Guyer, R. C. Richardson, and L. I. Zane, *Rev. Mod. Phys.* **43**, 532 (1971); E. R. Dobbs, *Helium Three* (Oxford University Press, Oxford, UK, 2000).

- [27] Y. Vekhov, W. J. Mullin, and R. B. Hallock, *Phys. Rev. Lett.* **113**, 035302 (2014).
- [28] Z. G. Cheng, J. Beamish, A. D. Fefferman, F. Souris, S. Balibar, and V. Dauvois, *Phys. Rev. Lett.* **114**, 165301 (2015).
- [29] Z. G. Cheng and J. Beamish, *Phys. Rev. Lett.* **117**, 025301 (2016).
- [30] D. Hull and D. Bacon, *Introduction to Dislocations*, 5th ed. (Butterworth-Heinemann, Oxford, UK, 2011).
- [31] E. J. Landinez Borda, W. Cai, and M. de Koning, *Phys. Rev. Lett.* **117**, 045301 (2016).